# Meteorology and Ozone, Temperature, Relative Humidity

J. Coates[1] and T. Butler[1]

[1]Institute for Advanced Sustainability Studies, Potsdam, Germany

November 1, 2015

**Abstract**

## 1 Introduction

Surface-level ozone ($O_3$) is a secondary air pollutant formed from the photochemical degradation of volatile organic compounds (VOCs) in the presence of nitrogen oxides ($NO_x$). Due to the photochemical nature of ozone production, meteorological factors such as temperature strongly influence ozone production (Jacob and Winner, 2009). Temperature influences ozone production through temperature-dependent emissions of VOC from biogenic sources (anthropogenic emissions are typically not temperature dependent) and the reaction rates of many of the chemical reactions involved in producing ozone are also temperature dependent. The recent review of Pusede et al. (2015) provides a detailed description of the temperature-dependent processes impacting ozone production.

Many studies over the US (Sillman and Samson, 1995), (Pusede et al., 2014) have observed the relationship between ozone and temperature, noting that increased temperatures tend to lead to higher ozone levels, often exceeding local air quality guidelines. Some of these studies include modelling experiments using regional chemical tranport models which have indeed verified the observed increases in ozone with temperature. The increase in the thermal decomposition rate of PAN (peroxy acetyl nitrate) with temperature is commonly cited for the increase of ozone with temperature.

choose proper citations

citations

Environmental chamber studies have looked at the relationship of ozone with temperature using a particular mixture of VOCs. The chamber experiments of Carter et al. (1979) and

Hatakeyama et al. (1991), also showed inreases in ozone with temperature and have also linked this relationship to increased PAN decomposition at higher temperatures (T >303 K). Hatakeyama et al. (1991) looked primarily at the influence of $HO_2NO_2$ decomposition on ozone production and induced that at lower temperatures (T < 303 K) $HO_2NO_2$ decomposition has a large influence on ozone production but the influence of PAN decomposition on ozone production increases with temperature.

Pusede et al. (2014) used observations over the San Joaquin Valley, California to infer a non-linear relationship of ozone production with temperature and $NO_x$, similar to the well-known non-linear relationship of ozone production on $NO_x$ and VOC levels (Sillman, 1999). In fact, Pusede et al. (2014) show that temperature can be used as a surrogate for VOC levels when looking at the relationship of ozone across $NO_x$ gradients. Moreover, the described relationship of ozone on both $NO_x$ and temperature needs to be considered when looking at effective stratgies to reduce levels of surface ozone.

Despite a wealth of studies looking at the effects of temperature on ozone chemistry, there have not been (to our knowledge) modelling studies focusing on these effects across different $NO_x$ gradients and whether the observed relationships are well-represented by different chemical mechanisms used in air quality models. The review of Pusede et al. (2015) also highlights a lack of modelling studies looking at this non-linear relationship of ozone on temperature across $NO_x$ gradients. In this study, we use an idealised box model to determine how ozone levels vary with temperature and across $NO_x$ gradients. We separate the effects of temperature-dependent chemistry and VOC emissions on ozone production by performing simulations including a temperature-independent source of isoprene followed by simulations using a temperature-dependent source of isoprene. Finally, by repeating these simulations with different chemical mechanisms, we determine whether the temperature dependence of ozone production is reproduced across different $NO_x$ gradients in these chemical mechanisms.

# 2 Methodology

## 2.1 Model Setup

- MECCA box model as described in Coates and Butler (2015) to broadly simulate the Benelux (Belgium, Netherlands and Luxembourg) region. As photolysis rates are parameterised by the solar zenith angle, the solar zenith angle of 51°N was used, representative of the central

Benelux region.

- MECCA box model has been updated to include vertical mixing with the free troposphere and accordingly includes a diurnal cycle for the PBL height. These amendments are discussed further in Sect. 2.4.

- Simulations start at 06:00 using spring equinoctical conditions and the simulations ended after two days.

- All simulations performed using the Master Chemical Mechanism, MCM v3.2, (Rickard et al., 2015), Common Representative Intermediates, CRI v2 (Jenkin et al., 2008), Model for Ozone and related chemical tracers, MOZART-4 (Emmons et al., 2010), Regional Acid Deposition Model, RADM2 (Stockwell et al., 1990) and the Carbon Bond Mechanism, CB05 (Yarwood et al., 2005). Coates and Butler (2015) describes the implementation of these chemical mechanisms for use with KPP within MECCA. These chemical mechanisms were chosen as they are commonly used by modelling groups and represent the highly-detailed chemistry (MCM v3.2), chemistry suitable for regional 3D models (CRI v2, RADM2 and CB05) and global 3D models (MOZART-4).

- NOx emissions and temperature were varied systematically to analyse the effects on ozone mixing ratios over different NOx gradients at each temperature.

- VOC emissions constant until noon of first day, to simulate a plume of emitted VOC.

- Two sets of runs were performed – to include both a temperature-dependent and temperature-independent source of biogenic VOC emissions. MEGANv2.1 (Guenther et al., 2012) was used to specify the temperature-dependent BVOC emissions of isoprene. Isoprene is the most important VOC at a global scale due its high emission rates and emissions from vegetation have been reported to depend on temperature (Guenther et al., 2006).

- Methane is fixed at 1.7 ppmv throughout the model run, carbon monoxide (CO) and ozone were initialised at 200 ppbv and 40 ppbv and then allowed to evolve freely throughout the the simulation.

- The temperature was systematically varied between 288 and 313 K (15 – 40 °C). The only source of NOx emissions in the box model was a constant source of NO emissions. The NO

emissions were systematically varied from $5.0 \times 10^9$ to $1.5 \times 10^{12}$ molecules (NO) $cm^{-2}$ $s^{-1}$ at each temperature used in this study.

## 2.2 VOC Emissions

- Anthropogenic emissions from Benelux for the year 2011 were obtained from the TNO-MACC_III emission inventory. TNO-MACC_III is the current version of the TNO-MACC_II inventory and was created using the same methodology as Kuenen et al. (2014) and based upon improvements to the existing emission inventory during the AQMEII-2 exercies described in Pouliot et al. (2015).

- Temperature-independent emissions of the biogenic VOC isoprene and monoterpenes, were calculated as a fraction of the total anthropogenic VOC emissions from each country in the Benelux region, this data was obtained from the supplementary data available from the EMEP (European Monitoring and Evaluation Programme) model (Simpson et al., 2012).

- AVOC and BVOC emissions are included as total emissions from SNAP (Selected Nomenclature for Air Pollution) source categories and these emissions were assigned to chemical groupings based on the country specific profiles for Belgium, the Netherlands and Luxembourg provided by TNO.

- The MCM v3.2 initial species were determined using the country specific profiles for each SNAP source category and where appropriate information of individual chemical species that can be represented by MCM v3.2 were determined using the detailed speciations of Passant (2002). This approach was also used in von Schneidemesser et al. (2015) and further details are found within this article.

- As in von Schneidemesser et al. (2015), first the primary VOC that are represented by the MCM v3.2 and respective emissions were determined. Using this MCM v3.2 data, the NMVOC emission data were mapped to mechanism species in the other four chemical mechanisms used in the study. The NMVOC emissions in the non-MCM v3.2 chemical mechanisms were weighted by the carbon numbers of the MCM v3.2 species and the emitted mechanism species. The supplementary data outlines the primary NMVOC and calculated emissions with each chemical mechanism.

Table 1: Total anthropogenic NMVOC emissions in 2011 in tonnes from each SNAP category assigned from TNO-MACC_III emission inventory and biogenic VOC emission in tonnes from Benelux region assigned from EMEP. The allocation of these emissions to MCM v3.2, CRI v2, CB05, MOZART-4 and RADM2 species is found in the supplement.

| | **SNAP1** | **SNAP2** | **SNAP34** | **SNAP5** | **SNAP6** | **SNAP71** |
|---|---|---|---|---|---|---|
| Belgium | 4494 | 9034 | 22152 | 5448 | 42809 | 6592 |
| Netherlands | 9140 | 12173 | 29177 | 8723 | 53535 | 16589 |
| Luxembourg | 121 | 44 | 208 | 1371 | 4482 | 1740 |
| Total | 13755 | 21251 | 62648 | 15542 | 100826 | 24921 |
| | **SNAP72** | **SNAP73** | **SNAP74** | **SNAP8** | **SNAP9** | **BVOC** |
| Belgium | 2446 | 144 | 210 | 6448 | 821 | 7042 |
| Netherlands | 3230 | 1283 | 1793 | 10067 | 521 | 1462 |
| Luxembourg | 1051 | 6 | 324 | 643 | 0 | 2198 |
| Total | 6727 | 1433 | 2327 | 17158 | 1342 | 10702 |

## 2.3 Temperature Dependent Isoprene Emissions

- Temperature dependent isoprene emissions were estimated using the MEGAN2.1 algorithm (Guenther et al., 2012).
- The aim of the study is to look at the effects of temperature, hence in the MEGAN2.1 algorithm all parameters (except temperature) were kept constant.
- The boxmodel setup uses a constant temperature throughout the model run and so the parameters $T_{24}$ and $T_{240}$, the average temperatures in the past 24 and 250 hours, were assumed to be constant and equal to the temperature value of the boxmodel.
- Constant PAR (photosynthetically active radiation) and LAI (leaf area index) were used at each temperature step.
- The LAI, plant functional type (PFT) and associated isoprene emission factor were taken from Guenther et al. (2012) and selected to give the same isoprene mixing ratios at a temperature of 293 K as in the temperature independent modelling case. For all other model runs over the different temperature, the MEGAN2.1 algorithm was used to estimate the isoprene emissions.
- Thus using this idealised case, we can determine the effects of increasing isoprene emissions with temperature across $NO_x$ gradients.
- This was repeated for each chemical mechanism.
- As in the temperature independent model runs, the emissions of NMVOC and the temperature dependent source of isoprene, were held constant until noon of the first day.
- Using these assumptions, the isoprene emissions at each temperature step of the study are illustrated in Fig. 1 and show the expected exponential increase in emissions with temperature (Guenther et al., 2006).

## 2.4 Vertical Mixing with Diurnal Boundary Layer Height

- The MECCA box model used in Coates and Butler (2015) included a constant boundary layer height of 1 km and no interactions (vertical mixing) with the free troposphere.

Figure 1: The estimated isoprene emissions (molecules isoprene $cm^{-2}$ $s^{-1}$) at each temperature step used in the study. Isoprene emissions were estimated using the MEGAN2.1 algorithm (Guenther et al., 2012).

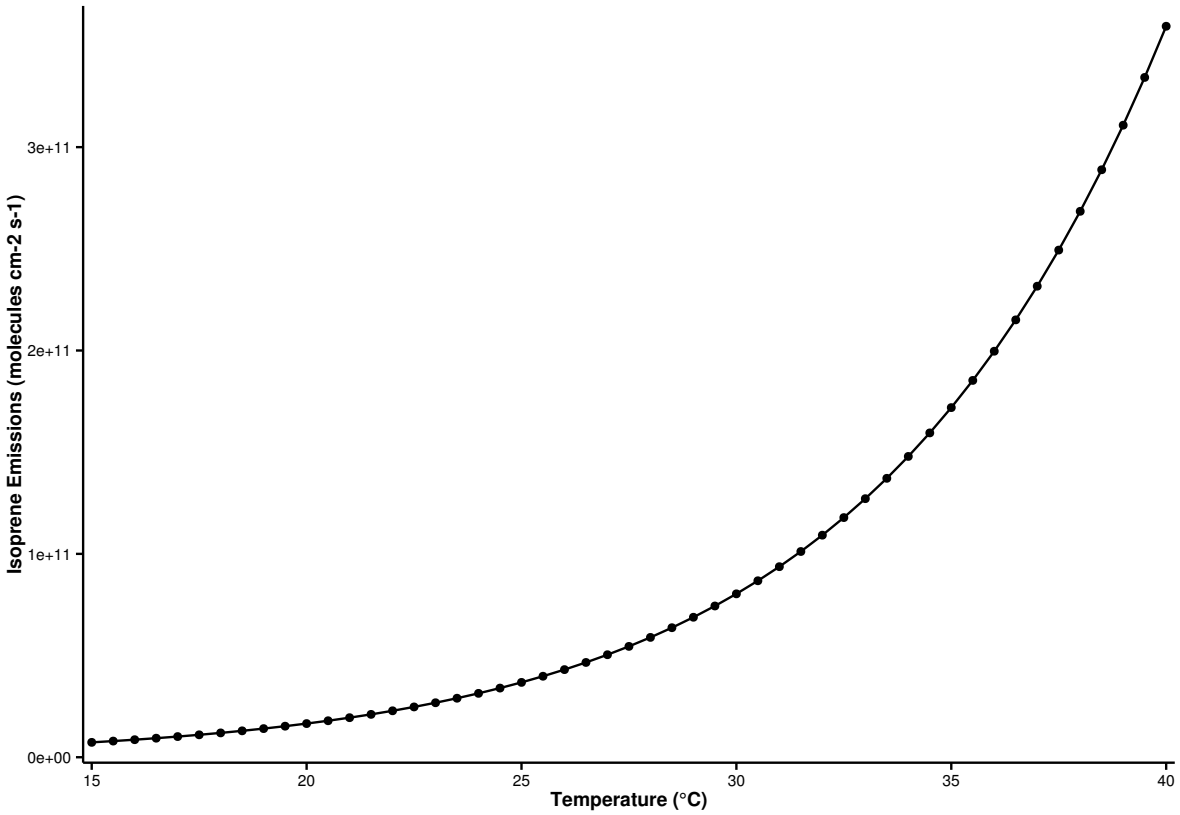

- The planetary boundary layer (PBL) height varies diurnally and affects chemistry by diluting emissions after sunrise when the PBL rises. The expansion of the PBL into the free troposphere introduces vertical mixing with those chemical species present in the free troposphere. When the PBL collapses in the evening, pollutants are trapped in the PBL.

- The mixing layer height was measured as part of the BAERLIN campaign over the city of Berlin, Germany. The profile of mean mixing layer height during the campaign period (June – August 2014) was used in the model to represent the diurnal cycle of the mixing layer height.

Reference Boris' paper

- The concentrations of the chemical species within the PBL are diluted due to the larger mixing volume when the PBL height increases at the beginning of the day, also the increasing PBL height mixes the chemical species from the free troposphere with the chemical species within the PBL i.e. vertical mixing. The PBL height collapses during night leaving the stable nocturnal boundary layer, trapping the chemical species into a smaller volume thus increasing the concentrations of the chemical species.

- This vertical mixing scheme was implemented into the boxmodel using the same approach of Lourens (2012).

- The mixing ratios of O3, CO and CH4 in the free troposphere were respectively set to 50 ppbv, 116 ppbv and 1.8 ppmv. These conditions were taken from the MATCH-MPIC chemical weather forecast model on the 21st March (the start date of the simulations). The model results (`http://cwf.iass-potsdam.de/`) at the 700 hPa height were chosen and the daily average was used as input into the boxmodel.

check reference

# 3 Results

## 3.1 Ozone mixing ratios as function of NOx and Temperature

Figure 2 depicts the maximum mixing ratio of ozone obtained from each model run as a function of the total $NO_x$ emissions on the first day and temperature. Using each mechanism, a similar non-linear relationship of ozone mixing ratios on $NO_x$ and temperature is found and increased ozone levels are found at higher temperatures when including a temperature-dependent source of isoprene emissions. CB05 and RADM2 produce the largest amount of ozone at higher temperatures than the other chemical mechanisms. A temperature-dependent source of isoprene,

Figure 2: Contours of maximum ozone mixing ratio as a function of the total $NO_x$ emissions on the first day and daily temperature for each chemical mechanism and using both a temperature-dependent and -independent source of isoprene emissions.

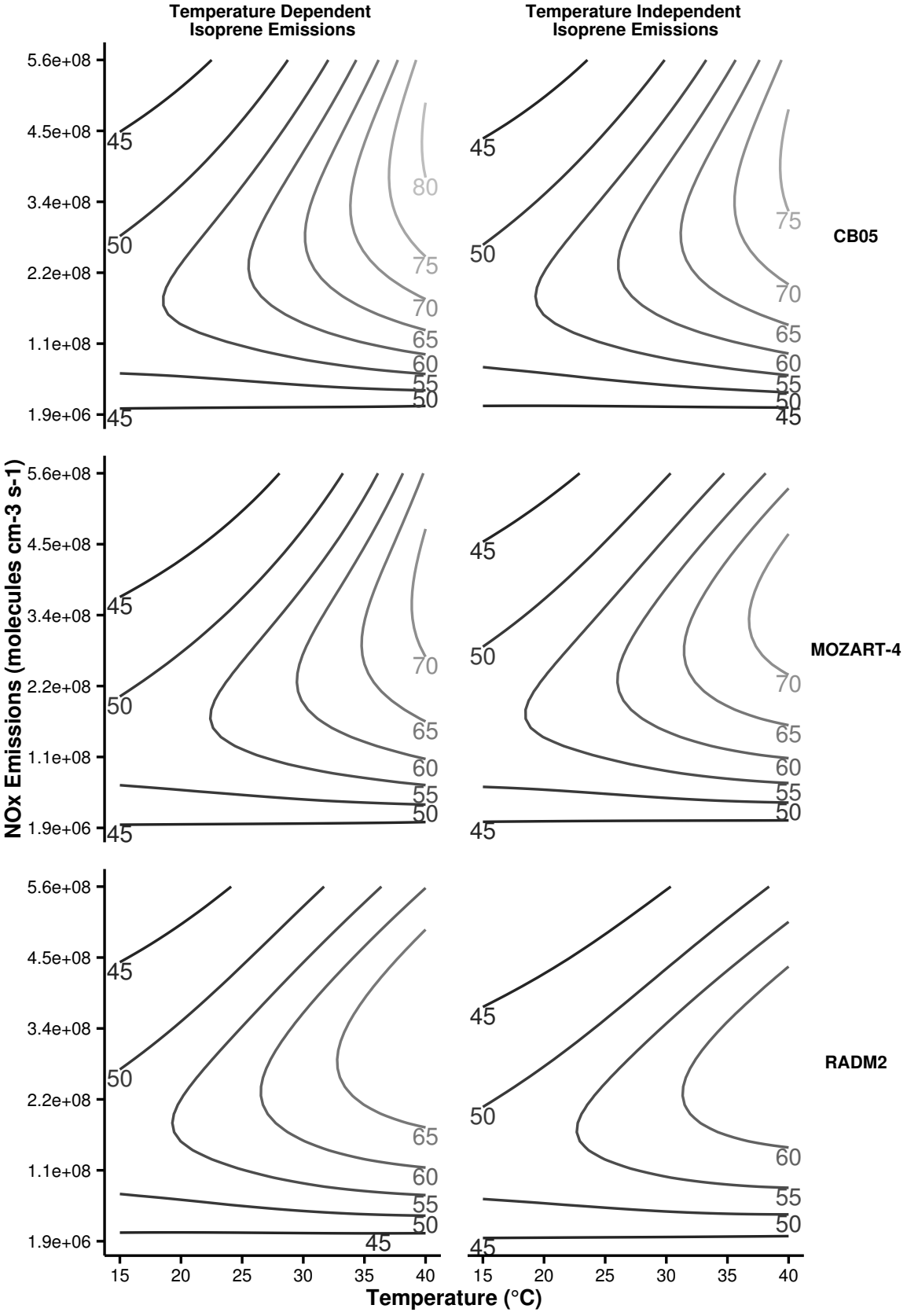

Table 2: Regression statistics for the linear relationship between ozone mixing ratios and temperature shown in Figure 3.

| Mechanism | NOx Condition | Temperature Dependent Isoprene Emissions | | Temperature Independent Isoprene Emissions | |
|---|---|---|---|---|---|
| | | Slope ($m_{O3\text{-}T}$) | $R^2$ | Slope ($m_{O3\text{-}T}$) | $R^2$ |
| CB05 | Low-NOx | 0.96 | 0.96 | 0.72 | 0.99 |
| | Maximal-O3 | 1.04 | 0.96 | 0.79 | 0.99 |
| | High-NOx | 1.07 | 0.96 | 0.81 | 0.99 |
| MOZART-4 | Low-NOx | 0.70 | 0.97 | 0.48 | 1.00 |
| | Maximal-O3 | 0.76 | 0.97 | 0.52 | 1.00 |
| | High-NOx | 0.78 | 0.97 | 0.53 | 1.00 |
| RADM2 | Low-NOx | 0.84 | 0.98 | 0.66 | 1.00 |
| | Maximal-O3 | 0.91 | 0.98 | 0.72 | 1.00 |
| | High-NOx | 0.92 | 0.98 | 0.72 | 1.00 |

leads to more efficient ozone production as at higher temperature a lower amount of $NO_x$ is required to produce the same amount of ozone as when using a temperature-independent source of isoprene. At low temperature and high $NO_x$, similar amounts of ozone are predicted from both the temperature-dependent and temperature-independent sources of isoprene emissions.

how? prove this

### 3.2 Rate of Change of Ozone with Temperature

Three $NO_x$ regimes–Low-NOx, High-NOx and Maximal-O3– are determined using the ratio of $H_2O_2$ to $HNO_3$, this ratio has been shown in Sillman (1995) to describe the different regimes of ozone production in relation to $NO_x$ and VOC levels. Values of $H_2O_2/HNO_3$ less than 0.3 correspond to the High-NOx regime, values larger than 0.5 correspond to the Low-NOx regime and all values inbetween correspond to the ridge area in which maximal ozone is produced. Each model run was allocated to one of the three regimes for each temperature and the mean ozone mixing ratio in these $NO_x$ regimes were then correlated with temperature as shown in Fig. 3. In literature, a linear relationship is typically reported between ozone and temperature and so the linear regression statistics are reported in Table 2.

The linear increase of ozone with temperature, $m_{O3\text{-}T}$ in Table 2, is highest at high-NOx conditions for each chemical mechanism and for each temperature case of isoprene emissions. The high-NOx regime corresponds to the top regions of the contour plots in Fig. 2 where increases in temperature would shift the ozone production towards the ridge of maximal ozone production, thus this increase in $m_{O3\text{-}T}$ is expected. Similarly, the lowest $m_{O3\text{-}T}$ are achieved in the low-NOx

Figure 3: Correlation of mean ozone mixing ratio with temperature in Low-NOx, maximal-O3 and High-NOx conditions for each chemical mechanism. A linear relationship between mean ozone mixing ratios and temperature is inferred, regression statistics are found in Table 2.

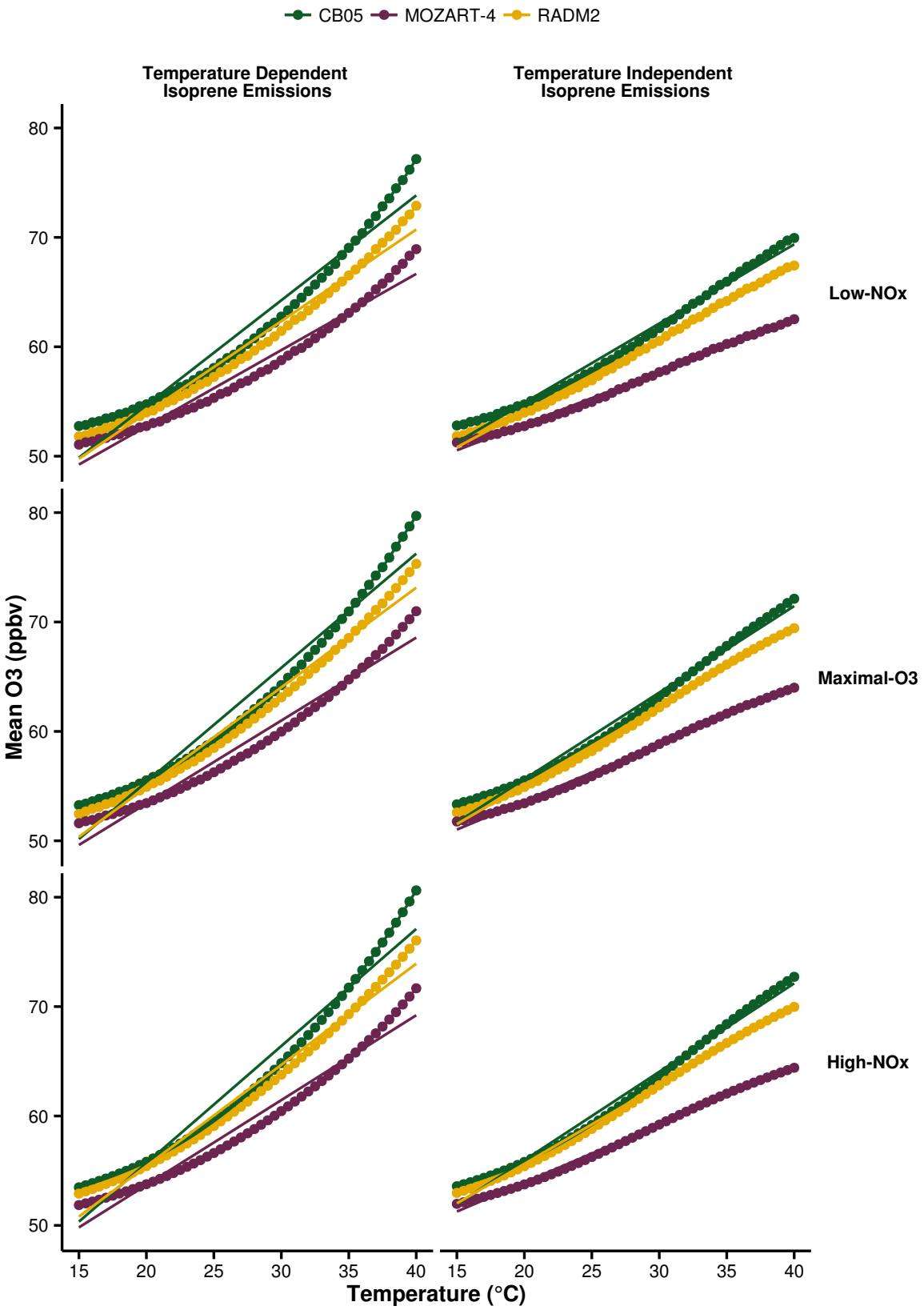

regime, the bottom regions of the contours in Fig. 2, where increases in temperature do not neccisarily lead to increased ozone levels.

# 4 Discussion

# 5 Conclusions

# References


William P. L. Carter, Arthur M. Winer, Karen R. Darnall, and James N. Pitts Jr. Smog chamber studies of temperature effects in photochemical smog. *Environmental Science & Technology*, 13 (9):1094–1100, 1979.

J. Coates and T. M. Butler. A comparison of chemical mechanisms using tagged ozone production potential (TOPP) analysis. *Atmospheric Chemistry and Physics*, 15(15):8795–8808, 2015.

L. K. Emmons, S. Walters, P. G. Hess, J.-F. Lamarque, G. G. Pfister, D. Fillmore, C. Granier, A. Guenther, D. Kinnison, T. Laepple, J. Orlando, X. Tie, G. Tyndall, C. Wiedinmyer, S. L. Baughcum, and S. Kloster. Description and evaluation of the Model for Ozone and Related chemical Tracers, version 4 (MOZART-4). *Geoscientific Model Development*, 3(1):43–67, 2010.

A. Guenther, T. Karl, P. Harley, C. Wiedinmyer, P. I. Palmer, and C. Geron. Estimates of global terrestrial isoprene emissions using MEGAN (Model of Emissions of Gases and Aerosols from Nature). *Atmospheric Chemistry and Physics*, 6(11):3181–3210, 2006.

A. B. Guenther, X. Jiang, C. L. Heald, T. Sakulyanontvittaya, T. Duhl, L. K. Emmons, and X. Wang. The Model of Emissions of Gases and Aerosols from Nature version 2.1 (MEGAN2.1): an extended and updated framework for modeling biogenic emissions. *Geoscientific Model Development*, 5(6):1471–1492, 2012.

Shiro Hatakeyama, Hajime Akimoto, and Nobuaki Washida. Effect of temperature on the formation of photochemical ozone in a propene-nitrogen oxide (nox)-air-irradiation system. *Environmental Science & Technology*, 25(11):1884–1890, 1991.

Daniel J. Jacob and Darrell A. Winner. Effect of climate change on air quality. *Atmospheric Environment*, 43(1):51 – 63, 2009. Atmospheric Environment - Fifty Years of Endeavour.

M.E. Jenkin, L.A. Watson, S.R. Utembe, and D.E. Shallcross. A Common Representative Intermediates (CRI) mechanism for VOC degradation. Part 1: Gas phase mechanism development. *Atmospheric Environment*, 42(31):7185 – 7195, 2008.

J. J. P. Kuenen, A. J. H. Visschedijk, M. Jozwicka, and H. A. C. Denier van der Gon. TNO-MACC_II emission inventory; a multi-year (2003–2009) consistent high-resolution european emission inventory for air quality modelling. *Atmospheric Chemistry and Physics*, 14(20): 10963–10976, 2014.

AsM Lourens. *Air quality in the Johannesburg-Pretoria megacity: its regional influence and identification of parameters that could mitigate pollution.* PhD thesis, North-West University, Potchefstroom Campus, 2012.

N. Passant. Speciation of UK emissions of non-methane volatile organic compounds. Technical report, DEFRA, Oxon, UK., 2002.

George Pouliot, Hugo A.C. Denier van der Gon, Jeroen Kuenen, Junhua Zhang, Michael D. Moran, and Paul A. Makar. Analysis of the emission inventories and model-ready emission datasets of Europe and North America for phase 2 of the AQMEII project. *Atmospheric Environment*, 115: 345–360, 2015.

S. E. Pusede, D. R. Gentner, P. J. Wooldridge, E. C. Browne, A. W. Rollins, K.-E. Min, A. R. Russell, J. Thomas, L. Zhang, W. H. Brune, S. B. Henry, J. P. DiGangi, F. N. Keutsch, S. A. Harrold, J. A. Thornton, M. R. Beaver, J. M. St. Clair, P. O. Wennberg, J. Sanders, X. Ren, T. C. VandenBoer, M. Z. Markovic, A. Guha, R. Weber, A. H. Goldstein, and R. C. Cohen. On the temperature dependence of organic reactivity, nitrogen oxides, ozone production, and the impact of emission controls in San Joaquin Valley, California. *Atmospheric Chemistry and Physics*, 14(7):3373–3395, 2014.

Sally E. Pusede, Allison L. Steiner, and Ronald C. Cohen. Temperature and Recent Trends in the Chemistry of Continental Surface Ozone. *Chemical Reviews*, 115(10):3898–3918, 2015.

Andrew Rickard, Jenny Young, M. J. Pilling, M. E. Jenkin, Stephen Pascoe, and S. M. Saunders. The Master Chemical Mechanism Version MCM v3.2. `http://mcm.leeds.ac.uk/MCMv3.2/`, 2015. [Online; accessed 25-March-2015].

Sanford Sillman. The use of noy, h2o2, and hno3 as indicators for ozone-nox -hydrocarbon sensitivity in urban locations. *Journal of Geophysical Research: Atmospheres*, 100(D7): 14175–14188, 1995.

Sanford Sillman. The relation between ozone, nox and hydrocarbons in urban and polluted rural environments. *Atmospheric Environment*, 33(12):1821 – 1845, 1999.

Sanford Sillman and Perry J. Samson. Impact of temperature on oxidant photochemistry in urban, polluted rural and remote environments. *Journal of Geophysical Research: Atmospheres*, 100(D6):11497–11508, 1995.

D. Simpson, A. Benedictow, H. Berge, R. Bergström, L. D. Emberson, H. Fagerli, C. R. Flechard, G. D. Hayman, M. Gauss, J. E. Jonson, M. E. Jenkin, A. Nyíri, C. Richter, V. S. Semeena, S. Tsyro, J.-P. Tuovinen, Á. Valdebenito, and P. Wind. The EMEP MSC-W chemical transport model – technical description. *Atmospheric Chemistry and Physics*, 12(16):7825–7865, 2012.

William R. Stockwell, Paulette Middleton, Julius S. Chang, and Xiaoyan Tang. The second generation regional acid deposition model chemical mechanism for regional air quality modeling. *Journal of Geophysical Research: Atmospheres*, 95(D10):16343–16367, 1990.

E. von Schneidemesser, J. Coates, A. J. H. Visschedijk, H. A. C. Denier van der Gon, and T. M. Butler. Variation of the NMVOC speciation in the solvent sector and the sensitivity of modelled tropospheric ozone. *Atmospheric Environment*, page In preparation, 2015.

Greg Yarwood, Sunja Rao, Mark Yocke, and Gary Z. Whitten. Updates to the Carbon Bond Chemical Mechanism: CB05. Technical report, U. S Environmental Protection Agency, 2005.